

# ESPRIT-Based Estimation of Location and Motion Dependent Parameters

Konstantinos Papakonstantinou and Dirk Slock  
Mobile Communications Department  
Eurecom  
Sophia Antipolis, France  
Email: papakons@eurecom.fr, slock@eurecom.fr

**Abstract**—The ESPRIT algorithm is an attractive solution to many parameter estimation problems due to its low computational cost. In this paper we apply ESPRIT to the estimation of the Angle of Arrivals (AoA), the Angle of Departures (AoD), the Delays and the Doppler Shifts of different components of the received signal. Due to the structure of the Channel Impulse Response Matrix of a MIMO-OFDM system, these four sets of parameters can be jointly estimated via a 4-dimensional algorithm, thus the need for pairing them is eliminated. The estimates of these parameters can essentially be utilized in localization algorithms applicable to Non-Line-of-Sight (NLoS) environments<sup>1</sup>.

## I. INTRODUCTION

Traditional geometrical localization techniques consist of the two following steps: First a set of location-dependent or location- and motion-dependent parameters (LMDP) are estimated in one or more Base Stations (BS). Widely used LMDP are the Angle of Arrival (AoA), the Angle of Departure (AoD), the delay or Time of Arrival (ToA), the Received Signal Strength (RSS) and the Doppler shift. Based on estimates of one or more of the above subsets of LMDP, the location of the Mobile Terminal (MT) can be derived either by solving a number of geometrical equations that its coordinates satisfy, or more often, for over-determined systems of equations, by finding the best candidate position that best fits the data (LMDP estimates) using a statistical approach like Maximum Likelihood (ML).

It is common practice in existing localization techniques, to assume that LMDP estimates are available. Thus, the performance is validated only for the second step. Examples of localization techniques that perform good in strictly NLoS environments can be found in [1] for static channels or [2] for dynamic channels. Both of these techniques are based on the Single-Bounce-Model (SBM), due to which an one-to-one invertible mapping between the LMDP of the NLoS signal components and the MT coordinates can be derived. In the former work, the authors consider knowledge of AoA, AoD and delays of all the signal components, while in the latter the authors also consider knowledge of the Doppler shifts.

<sup>1</sup>Eurecom's research is partially supported by its industrial members: BMW Group Research & Technology, Bouygues Telecom, Cisco, Hitachi, ORANGE, SFR, Sharp, STMicroelectronics, Swisscom, Thales. The work presented in this paper has also been partially supported by the European FP7 projects Where and Newcom++ and by the French ANR project Semafor.

In this work, we focus on the first step of localization. We consider a Multiple-Input Multiple-Output (MIMO) system, a MT that moves so that its signal is affected by Doppler frequency shifts and an OFDM signal that propagates through a NLoS propagation environment. We parameterize the channel impulse response (CIR) matrix in such a way, that a 4-dimensional (4-D) ESPRIT algorithm can be utilized to jointly estimate 4 subsets of LMDP, namely the AoA, the AoD, the delays and the Doppler Shifts. If we assume that the MT is not moving, then the problem can be easily reformulated, so that a 3-D ESPRIT algorithm can jointly estimate the AoA, the AoD and the delays of the NLoS paths. Therefore, the work presented herein can be used as a complement to the techniques in [1] and [2], to form a complete localization procedure.

ESPRIT algorithm<sup>2</sup> was introduced in [3] as a computationally attractive estimation algorithm that exploits the rotational invariance of the signal subspace. Its impact was such that many contributions followed. The algorithm was extended to the 2-D case in [4] and [5] and to a multidimensional case in [6]. An algorithm with superior performance and reduced computational cost, called Unitary ESPRIT, was introduced in [7] and extended to the multidimensional case in [8]. Finally a 2-D Unitary ESPRIT for MIMO systems was introduced in [9]. The proposed 4-D ESPRIT closely follows the guidelines in these two last papers.

**Notation:** Throughout the paper, upper case and lower case boldface letters will represent matrices and column vectors respectively. If an upper case boldface letter has been utilized to represent a matrix (eg.  $\mathbf{A}$ ), the lower case of the same letter will always correspond to the vectorized form of that matrix, i.e.  $\mathbf{a} = \text{vec}(\mathbf{A}) \triangleq [\mathbf{a}_1^t, \dots, \mathbf{a}_N^t]^t$ .  $(\cdot)^t$  will denote the transpose,  $(\cdot)^*$  the conjugate and  $(\cdot)^\dagger$  the conjugate transpose of any vector or matrix.  $(\cdot)^+$  will denote the pseudoinverse of a matrix. For a square  $M \times M$  matrix  $\mathbf{A}$ ,  $\text{diag}(\mathbf{A})$  is a  $M \times 1$  vector composed from its diagonal entries  $a_{ii}, 1 \leq i \leq M$ , while for a  $M \times 1$  vector  $\mathbf{a} = [a_1, \dots, a_M]^t$ ,  $\text{diag}(\mathbf{a})$  is an  $M \times M$  diagonal matrix with  $\mathbf{a}$ 's entries along its main diagonal. The symbols  $\otimes$ ,  $\boxtimes$  and  $\odot$  denote the Kronecker, Khatri-Rao (column-wise Kronecker) and Hadamard product

<sup>2</sup>ESPRIT stands for "Estimation of Signal Parameters via Rotational Invariance Techniques"

respectively.

## II. CHANNEL MODEL

The SBM has been used extensively to describe the NLoS paths of a multipath propagation environment. It is based on the realistic assumption that the first few arriving signal components have bounced only once while propagating through the wireless channel. It enables the derivation of simple equations that express the LMDP as functions of the coordinates and the speed of the MT. Thus, it can be used in localization algorithms. Furthermore, due to the fact that it assigns one parameter from each subset of LMDP to each path (or scatterer or signal component)<sup>3</sup> it simplifies the expressions used to describe the CIR Matrix and thus can also be applied in statistical channel modeling. An example of a SBM with two paths has been drawn in 1, where  $\psi$ s denote the AOD and  $\phi$ s denote the AOA.

The discrete input-output relationship of a  $n_r \times n_t$  MIMO-OFDM system in the time-frequency domain, is:

$$\mathbf{Y}_{i_f i_t} = \mathbf{H}_{i_f i_t} \mathbf{X}_{i_f i_t} + \mathbf{N}_{i_f i_t} \quad (1)$$

where  $\mathbf{X}_{i_f i_t}$  is the  $n_t \times N$  transmitted signal matrix,  $N$  is the number of OFDM symbols,  $\mathbf{Y}_{i_f i_t}$  is the  $n_r \times N$  received signal matrix and  $\mathbf{N}_{i_f i_t}$  is the  $n_r \times N$  noise matrix,  $\forall i_f \in \{0, 1, \dots, (N_f - 1)\}$  and  $\forall i_t \in \{0, 1, \dots, (N_t - 1)\}$ . To work directly with received signals, we will assume that the pilot symbols used in this estimation process are the same  $\forall \{i_f, i_t\}$ , i.e.  $\mathbf{X}_{i_f i_t} = \mathbf{X}$ . If this condition is not met, estimates of the CIR matrix are required to serve as a starting point for the ESPRIT algorithm presented in the following sections.

For a NLOS environment that can be accurately described by the SBM, the channel matrix  $\mathbf{H}_{i_f i_t}$  is given by<sup>4</sup> [10], [11]:

$$\begin{aligned} \mathbf{H}_{i_f i_t} &= \frac{1}{\sqrt{P_{tot}}} \sum_{i=1}^{N_s} \sqrt{P_i} \gamma_i e^{j2\pi i_t \Delta t f_{d,i}} \mathbf{a}_R(\phi_i) \mathbf{a}_T^t(\psi_i) \\ &\quad H_{TR} e^{-j2\pi i_f \Delta f \tau_i} \\ &= \mathbf{A}_R (\mathbf{\Gamma} \odot (\mathbf{D}_{i_f} \mathbf{F}_{d,i_t})) \mathbf{A}_T^t = \mathbf{A}_R \mathbf{\Gamma} \mathbf{D}_{i_f} \mathbf{F}_{d,i_t} \mathbf{A}_T^t. \end{aligned} \quad (2)$$

where  $\Delta t$  and  $\Delta f$  are the sampling intervals in time and frequency respectively. In the above equation we have introduced the delays,  $\tau_i$ , the Doppler shifts,  $f_{d,i}$ , the complex amplitudes  $\gamma_i$  and the powers,  $P_i = \tau_i^{-2}$ , of the  $N_s$  signal components along with the normalization constant  $P_{tot}$  which contains all the common to the different powers, constant terms. We further introduced the  $n_r \times 1$  and  $n_t \times 1$  array responses  $\mathbf{a}_R(\phi_i)$  and  $\mathbf{a}_T(\psi_i)$  of the receiver and the transmitter respectively, for the signal component with AOA  $\phi_i$  and AOD  $\psi_i$ . For sake of simplicity, we will assume Uniform Linear Arrays (ULA) at both ends of the communication link, so that

$$\mathbf{a}_R(\phi_i) = [1, e^{j2\pi \frac{f_c}{c} d_r \sin(\phi_i)}, \dots, e^{j2\pi \frac{f_c}{c} d_r (n_r - 1) \sin(\phi_i)}]^t \quad (3)$$

<sup>3</sup>In fact one discrete object (scatterer), which corresponds to one signal component, is used to describe a mini cluster of very closely spaced scatterers.

<sup>4</sup>The proposed channel matrix representation is also valid for any NLOS environment where each AOA is linked with one AOD but not necessarily via a single scatterer.

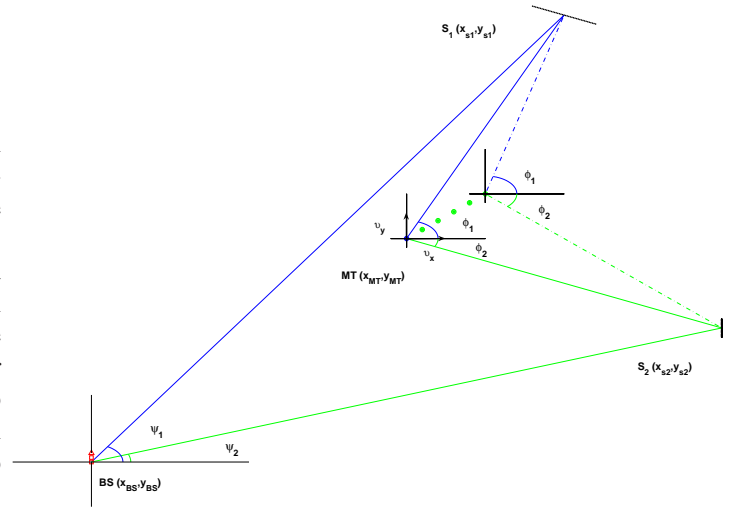


Fig. 1. Single Bounce model

and  $\mathbf{a}_T(\psi_i)$  is given by replacing  $\phi_i$  by  $\psi_i$ ,  $n_r$  by  $n_t$  and the distance between two consecutive elements,  $d_r$ , by  $d_t$ . Any general array that can be decomposed into 2 subarrays with identical elements separated by  $d$  can be considered instead.  $H_{TR} = FT\{h_{TR}(\tau)\}$  is the transfer function of the cascade of the filters at the transmitter's and receiver's front end. It should be noted that although the LMDP considered above are all time-varying due to the movement of the MT, they will be treated as constants, since their variation for a small observation time (of the order of msec) is negligible. The newly introduced matrices on the r.h.s. of eq. (2) are defined as follows

$$\mathbf{A}_R \triangleq [\mathbf{a}_R(\phi_1), \dots, \mathbf{a}_R(\phi_{N_s})] \quad (4)$$

$$\mathbf{A}_T \triangleq [\mathbf{a}_T(\psi_1), \dots, \mathbf{a}_T(\psi_{N_s})] \quad (5)$$

$$\mathbf{\Gamma} \triangleq H_{TR} \text{diag}(\gamma) \quad (6)$$

$$\mathbf{D}_{i_f} \triangleq \text{diag}(\mathbf{d}_{i_f}) \quad (7)$$

$$\mathbf{F}_{d,i_t} \triangleq \text{diag}(\mathbf{f}_{d,i_t}) \quad (8)$$

where

$$\gamma \triangleq \frac{1}{\sqrt{P_{tot}}} \text{diag}([\sqrt{P_1} \gamma_1, \dots, \sqrt{P_{N_s}} \gamma_{N_s}]) \quad (9)$$

$$\mathbf{d}_{i_f} \triangleq [e^{-j2\pi i_f \Delta f \tau_1}, \dots, e^{-j2\pi i_f \Delta f \tau_{N_s}}] \quad (10)$$

$$\mathbf{f}_{d,i_t} \triangleq [e^{j2\pi i_t \Delta t f_{d,1}}, \dots, e^{j2\pi i_t \Delta t f_{d,N_s}}]. \quad (11)$$

## III. DATA PREPROCESSING FOR 4-D ESPRIT

In order to implement the 4-D Unitary ESPRIT algorithm and estimate the AOA, AOD, delays and Doppler shifts directly from the received signal samples, we need to rewrite the input-output relationship in a form such that the CIR matrix inherits a shift invariance property in all four dimensions. The following 4 steps are required to achieve that.

1. Split the set of the  $N_f N_t$  received matrices (samples) into  $L = L_f L_t$  subsets  $\mathbb{S}_{l_f, l_t}$  of  $M = M_f M_t$  samples each. Assuming that the subsets  $\mathbb{S}_{l_f, L_t}$ ,  $1 \leq l_f \leq L_f$  and  $\mathbb{S}_{L_f, l_t}$ ,  $1 \leq l_t \leq L_t$  are padded with zero matrix entries if necessary,

$M_f = \left\lceil \frac{N_f}{L_f} \right\rceil$  and  $M_t = \left\lceil \frac{N_t}{L_t} \right\rceil$ . This separation of the data is equivalent to a smoothing that ensures that more than one measurement vector will be used in the final formulation.

2. Vectorize the receive signal matrices, so that the  $n_r n_t \times 1$  received signal vectors  $\mathbf{y}_{i_f i_t}$  is given by:

$$\mathbf{y}_{i_f i_t} = \mathbf{h}_{i_f i_t} + \mathbf{n}_{i_f i_t} \quad (12)$$

$$\mathbf{h}_{i_f i_t} \triangleq (\mathbf{X}^t \mathbf{A}_T \boxtimes \mathbf{A}_R) \mathbf{\Gamma} \mathbf{F}_{d,1}^{(l_t-1)} \mathbf{D}_{i_f} \mathbf{f}_{d,m_t} \quad (13)$$

where  $l_t = \left\lfloor \frac{i_t}{M_t} \right\rfloor$  and  $m_t = l_t - \left\lfloor \frac{i_t}{M_t} \right\rfloor M_t$ .

3. For each of the subsets, i.e. for  $1 \leq l_f \leq L_f$  and  $1 \leq l_t \leq L_t$ , do the following concatenations and vectorizations:

3a. Stack the column vectors  $\mathbf{y}_{i_f i_t}$ ,  $(l_t - 1)M_t + 1 \leq i_t \leq l_t M_t$  of the corresponding subset  $\mathbb{S}_{L_f, l_t}$  to form matrix  $\bar{\mathbf{Y}}_{i_f l_t}$  of size  $n_r n_t \times M_t$  and vectorize again to get:

$$\bar{\mathbf{y}}_{i_f l_t} = \bar{\mathbf{h}}_{i_f l_t} + \bar{\mathbf{n}}_{i_f l_t} \quad (14)$$

$$\bar{\mathbf{h}}_{i_f l_t} \triangleq (\mathbf{F}_{d,1:M_t}^t \boxtimes \mathbf{X}^t \mathbf{A}_T \boxtimes \mathbf{A}_R) \bar{\mathbf{\Gamma}}_{l_f l_t} \mathbf{d}_{m_f} \quad (15)$$

$$\mathbf{F}_{d,1:M_t}^t \triangleq [\mathbf{f}_{d,1}, \dots, \mathbf{f}_{d,M_t}] \quad (16)$$

$$\bar{\mathbf{\Gamma}}_{l_f l_t} \triangleq \mathbf{\Gamma} \mathbf{F}_{d,1}^{(l_t-1)} \mathbf{D}_1^{(l_f-1)} \quad (17)$$

where  $l_f = \left\lfloor \frac{i_f}{M_f} \right\rfloor$  and  $m_f = l_f - \left\lfloor \frac{i_f}{M_f} \right\rfloor M_f$ .

3b. In a similar way, stack the column vectors  $\mathbf{y}_{i_f l_t}$ ,  $(l_f - 1)M_f + 1 \leq i_f \leq l_f M_f$  to form  $L = L_f L_t$  matrices  $\bar{\mathbf{Y}}_{l_f l_t}$  and vectorize again to get:

$$\bar{\bar{\mathbf{y}}}_{l_f l_t} = \bar{\bar{\mathbf{H}}}_{l_f l_t} \bar{\bar{\boldsymbol{\gamma}}}_{l_f l_t} + \bar{\bar{\mathbf{n}}}_{l_f l_t} \quad (18)$$

$$\bar{\bar{\mathbf{H}}} \triangleq (\mathbf{D}_{1:M_f}^t \boxtimes \mathbf{F}_{d,1:M_t}^t \boxtimes \mathbf{X}^t \mathbf{A}_T \boxtimes \mathbf{A}_R) \quad (19)$$

$$\mathbf{D}_{1:M_f}^t \triangleq [\mathbf{d}_{(i-1)M_t+1}, \dots, \mathbf{d}_{iM_t}] \quad (20)$$

$$\bar{\bar{\boldsymbol{\gamma}}}_{l_f l_t} \triangleq (\mathbf{D}_1^{(l_f-1)}) \odot \mathbf{F}_{d,1}^{(l_t-1)} \boldsymbol{\gamma} \quad (21)$$

4. Stack all generated vectors in a big matrix

$$\begin{aligned} \bar{\bar{\mathbf{Y}}} &= [\bar{\bar{\mathbf{y}}}_{11}, \dots, \bar{\bar{\mathbf{y}}}_{L_f L_t}] \\ &= \bar{\bar{\mathbf{H}}} \bar{\bar{\boldsymbol{\Gamma}}} + \bar{\bar{\mathbf{N}}} \end{aligned} \quad (22)$$

where we have introduced

$$\bar{\bar{\boldsymbol{\Gamma}}} = [\bar{\boldsymbol{\gamma}}_{11}, \dots, \bar{\boldsymbol{\gamma}}_{L_f L_t}] \quad (23)$$

$$\bar{\bar{\mathbf{N}}} = [\bar{\mathbf{n}}_{11}, \dots, \bar{\mathbf{n}}_{L_f L_t}]. \quad (24)$$

It should be noted that this type of formulation is possible due to the fact that  $\mathbf{\Gamma}$ ,  $\mathbf{D}_k$  and  $\mathbf{F}_{d,l}$  are diagonal, which in turn is a consequence of the fact that each path is distinct. Also it becomes obvious that the matrix  $\bar{\bar{\boldsymbol{\Gamma}}}$  and not the original transmitted matrix  $\mathbf{X}$  plays the role of the unknown signal in our model.

#### IV. 4-D ESPRIT FOR JOINT AOA, AOD, DELAY AND DOPPLER SHIFT ESTIMATION

A simple, yet efficiency way to increase the number of the data used in the estimation process, while simultaneously decrease the computational cost, is to transform  $\bar{\bar{\mathbf{Y}}}$  into a

centro-Hermitian matrix and subsequently into a real matrix<sup>5</sup>, to get:

$$\bar{\bar{\mathbf{Y}}}_r = \mathbf{Q}_{\text{MN}}^\dagger [\bar{\bar{\mathbf{Y}}} \mathbf{\Pi}_{\text{MN}} \bar{\bar{\mathbf{Y}}}^* \mathbf{\Pi}_L] \mathbf{Q}_{2L} \quad (25)$$

where  $\mathbf{\Pi}$  are permutation matrices obtained by reversing the order of the rows of  $\mathbf{I}$  and  $\mathbf{Q}$  are left  $\mathbf{\Pi}$ -real matrices. A common example of left  $\mathbf{\Pi}$ -real matrix is

$$\mathbf{Q} = \frac{1}{\sqrt{2}} \begin{bmatrix} \mathbf{I}_q & \mathbf{0} & j\mathbf{I}_q \\ \mathbf{0}^t & \sqrt{2} & \mathbf{0}^t \\ \mathbf{\Pi}_q & \mathbf{0} & -j\mathbf{\Pi}_q \end{bmatrix} \quad (26)$$

for odd sizes, or by deleting the center row and column, one can get the equivalent for even sizes. Due to the noise term on the r.h.s. of eq. (22),  $\bar{\bar{\mathbf{Y}}}_r$  is full rank, instead of rank  $N_s$ . This affects the solution of any ESPRIT algorithm, by resulting in a number of estimates that is greater than the number of parameters that need to be estimated. To mitigate this, a rank reduction can be performed, using for example the SVD decomposition of  $\bar{\bar{\mathbf{Y}}}_r$ . From the SVD, the  $N_s$  dominant left singular vectors, composing  $\mathbf{E}_{N_s}$ , can be derived. These vectors span the signal subspace and thus  $\mathbf{E}_{N_s}$  can be used to form the invariance equations in all four dimensions. Specifically, let  $r$  denote one of the four dimensions of the rotational invariant matrix  $\bar{\bar{\mathbf{H}}}$  and let  $N_r$  denote one of the corresponding number of data  $\{n_r, n_t, M_t, M_f\}$ , on each of these dimensions. Following the reasoning behind the ESPRIT algorithm, it is easy to show that

$$\mathbf{K}_{N_r,1} \mathbf{E}_{N_s} \boldsymbol{\Theta}_r = \mathbf{K}_{N_r,2} \mathbf{E}_{N_s} \quad (27)$$

where the matrices denoted by  $\mathbf{K}_{N_r,i}$ ,  $i = 1, 2$  are constructed by transforming the selection matrices denoted by  $\mathbf{J}_{N_r}$ , according to

$$\mathbf{K}_{N_r,1} = 2\text{Re}\{\mathbf{Q}_{N_r}^\dagger \mathbf{J}_{N_r} \mathbf{Q}_L\} \quad (28)$$

$$\mathbf{K}_{N_r,2} = 2\text{Im}\{\mathbf{Q}_{N_r}^\dagger \mathbf{J}_{N_r} \mathbf{Q}_L\} \quad (29)$$

and the 4 selection matrices are given by

$$\mathbf{J}_{n_r} = \mathbf{I}_{M_f} \otimes \mathbf{I}_{M_t} \otimes \mathbf{I}_{n_t} \otimes [\mathbf{0}_{(n_r-1) \times 1} \mathbf{I}_{n_r-1}] \quad (30)$$

$$\mathbf{J}_{n_t} = \mathbf{I}_{M_f} \otimes \mathbf{I}_{M_t} \otimes [\mathbf{0}_{(n_t-1) \times 1} \mathbf{I}_{n_t-1}] (\mathbf{X}^t)^\dagger \otimes \mathbf{I}_{n_r} \quad (31)$$

$$\mathbf{J}_{M_t} = \mathbf{I}_{M_f} \otimes [\mathbf{0}_{(M_t-1) \times 1} \mathbf{I}_{M_t-1}] \otimes \mathbf{I}_{n_t} \otimes \mathbf{I}_{n_r} \quad (32)$$

$$\mathbf{J}_{M_f} = [\mathbf{0}_{(M_f-1) \times 1} \mathbf{I}_{M_f-1}] \otimes \mathbf{I}_{M_t} \otimes \mathbf{I}_{n_t} \otimes \mathbf{I}_{n_r}. \quad (33)$$

The Invariance equations given by eq. (27) can be solved by means of Least-Squares (LS) or any of its more advanced variants, to obtain the matrices  $\boldsymbol{\Theta}_r$ . The LS solution yields

$$\boldsymbol{\Theta}_r = (\mathbf{K}_{N_r,1} \mathbf{E}_{N_s})^\dagger \mathbf{K}_{N_r,2} \mathbf{E}_{N_s} \quad (34)$$

where  $(\mathbf{K}_{N_r,1} \mathbf{E}_{N_s})^\dagger$  is

$$(\mathbf{K}_{N_r,1} \mathbf{E}_{N_s})^\dagger = ((\mathbf{K}_{N_r,1} \mathbf{E}_{N_s})^t \mathbf{K}_{N_r,1} \mathbf{E}_{N_s})^{-1} (\mathbf{K}_{N_r,1} \mathbf{E}_{N_s})^t \quad (35)$$

while the Total Least-Squares (TLS) solution yields

$$\boldsymbol{\Theta}_r = -\mathbf{V}_{12} \mathbf{V}_{22}^{-1} \quad (36)$$

<sup>5</sup>This transformation forces the solutions of the algorithm to lie on the unit circle and thus the name "Unitary ESPRIT"

where  $\mathbf{V}_{12}$  and  $\mathbf{V}_{22}$  are the upper right and lower right  $N_s \times N_s$  submatrices of  $\mathbf{V}$ , which in turn is obtained from the SVD of  $[\mathbf{K}_{N_r,1}\mathbf{E}_{N_s} \ \mathbf{K}_{N_r,2}\mathbf{E}_{N_s}]$ , i.e.

$$[\mathbf{K}_{N_r,1}\mathbf{E}_{N_s} \ \mathbf{K}_{N_r,2}\mathbf{E}_{N_s}] = \mathbf{U}\mathbf{\Sigma}\mathbf{V}^\dagger. \quad (37)$$

From these matrices we can derive the LMDP estimates as follows. Define  $\mathbf{\Omega}_r$ ,  $r = 1, \dots, 4$  the  $N_s \times N_s$  diagonal matrices with diagonal entries

$$\omega_{i1} = \tan\left(\frac{2\pi \frac{f_c}{c} d_r \sin(\phi_i)}{2}\right), \quad r = 1 \quad (38)$$

$$\omega_{i2} = \tan\left(\frac{2\pi \frac{f_c}{c} d_t \sin(\psi_i)}{2}\right), \quad r = 2 \quad (39)$$

$$\omega_{i3} = \tan\left(\frac{-2\pi i_f \Delta f \tau_i}{2}\right), \quad r = 3 \quad (40)$$

$$\omega_{i4} = \tan\left(\frac{2\pi i_t \Delta t f_{d,i}}{2}\right), \quad r = 4. \quad (41)$$

Each matrix  $\mathbf{\Omega}_r$  contains the  $N_s$  eigenvalues of the corresponding  $\mathbf{\Theta}_r$ . Thus, if  $\mathbf{\Theta}_r$  are available, one needs to compute their eigenvalues and then use the above equations to get the LMDP estimates. To avoid the need for pairing the estimates, joint diagonalization or triangularization is highly recommended, since it can achieve automatic pairing. This is a direct consequence of the fact that the four  $\mathbf{\Theta}_r$  share the same set of eigenvectors in the absence of noise. In the presence of noise, these sets are approximately the same. Following the work in [8], Simultaneous Schur Decomposition (SSD) will be utilized to compute the eigenvalues of the four  $\mathbf{\Theta}_r = \mathbf{B}\mathbf{R}_r\mathbf{B}^t$ .

The SSD is an iterative procedure that tries to derive approximate upper triangular matrices simultaneously. Each iteration has  $\frac{1}{2}N_s(N_s - 1)$  steps. It starts with  $\mathbf{R}_{r,0} = \mathbf{\Theta}_r$ ,  $r = 1, \dots, 4$  and in each step  $j$  the matrices  $\mathbf{R}_{r,j}$ , are updated as follows

$$\mathbf{R}_{r,j} = \mathbf{B}_{i_1 i_2}^t \mathbf{R}_{r,j-1} \mathbf{B}_{i_1 i_2} \quad (42)$$

where the elementary Jacobi rotation matrix  $\mathbf{B}_{i_1 i_2}(\alpha)$  is chosen to minimize the following cost function

$$e(\mathbf{B}_{i_1 i_2}) = \sum_{r=1}^4 \|\mathcal{L}(\mathbf{R}_{r,j})\|^2 = \text{tr}\left\{\sum_{r=1}^4 \mathcal{L}(\mathbf{R}_{r,j})\mathcal{L}(\mathbf{R}_{r,j})^t\right\} \quad (43)$$

$\mathcal{L}$  denotes the strictly lower triangular part of a matrix. These Jacobi matrices are constructed from identity matrices, by replacing four of their entries as follows

$$\beta_{i_1 i_2} = -\beta_{i_2 i_1} = \sin(\alpha) \quad (44)$$

$$\beta_{i_1 i_1} = \beta_{i_2 i_2} = \cos(\alpha). \quad (45)$$

It is obvious that finding the matrix  $\mathbf{B}_{i_1 i_2}(\alpha)$  that minimizes  $e(\mathbf{B}_{i_1 i_2})$  in each step is equivalent to finding  $\alpha$ . The solution to this problem was given in [8]. After the  $\frac{1}{2}N_s(N_s - 1)$  steps have been completed, the final matrices  $\mathbf{R}_{r, \frac{1}{2}N_s(N_s - 1)}$  serve as starting points  $\mathbf{R}_{r,0}$  and the operation can be repeated to yield matrices that are even closer to upper triangular. After just a few iterations, the algorithm outputs  $\mathbf{I}$  as the Jacobi matrix in each step and thus the cost function can not be minimized further.

TABLE I  
MT AND SCATTERERS' COORDINATES

$(x_{MT}, y_{MT})$	$(x_{s1}, y_{s1})$	$(x_{s2}, y_{s2})$	$(x_{s3}, y_{s3})$	$(x_{s4}, y_{s4})$
(30, 20)m	(20, 30)m	(35, 20)m	(40, 15)m	(15, 25)m

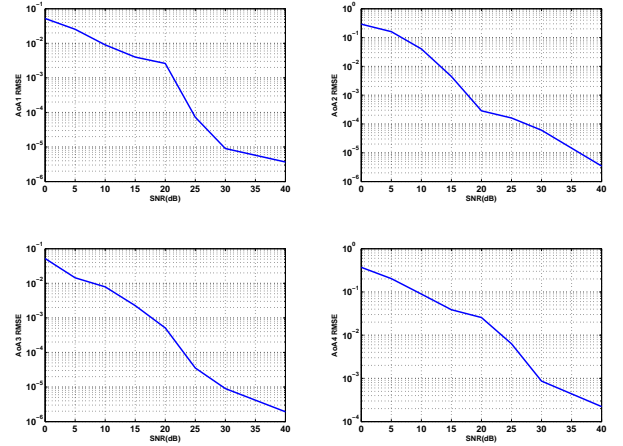


Fig. 2. RMSE of  $\sin(\phi)$

## V. NUMERICAL EXAMPLES

In this section we evaluate the performance of the proposed method in terms of the RMSE of the LMDP estimates. We will assume that the transmitter's ULA is equipped with four antenna elements and the receiver's ULA is equipped with only two. The transmitted signal propagates through  $N_s = 4$  distinct NLoS paths. The coordinates of the corresponding four scatterers along with the coordinates of the MT are given in table I. The BS is assumed to be placed at the origin. The magnitude of the speed of the MT is  $|v| = 1.5\text{m/sec}$  (average walking speed) and the direction is  $-\frac{\pi}{3}$ .  $N_t = 40$  time samples with  $\Delta t = 1\text{msec}$  and  $N_f = 8$  frequency samples with  $\Delta f = 10\text{MHz}$  are considered. The impact of the choice of the data smoothing numbers,  $L_t$  and  $L_f$ , on the estimates of the different LMDP was studied. The results indicated that there is a trade-off between performance for different subsets of LMDP, rather than some optimal smoothing numbers that minimize RMSE for all of them. The only restriction on the smoothing numbers is that their product must satisfy  $L \geq N_s$ , so that the LMDP become identifiable. The results shown in the figures correspond to  $L_f = 2$  and  $L_t = 8$ . On a similar basis, for identifiability purposes, the largest of the four dimensions  $N_r$  must satisfy

$$\prod_{r=1}^4 N_r \frac{N_{r,max} - 1}{N_{r,max}} \geq N_s. \quad (46)$$

The carrier frequency is  $f_c = 1.9\text{GHz}$  and the transmitted pilot signal is the training matrix  $\mathbf{X} = \mathbf{I}$ . We run  $N = 50$  independent trials and averaged the results, thus the RMSE is

$$RMSE(\mu_{ir}) = \sqrt{\frac{1}{N} \sum_{n=1}^N |\hat{\mu}_{ir} - \mu_{ir}|^2} \quad (47)$$

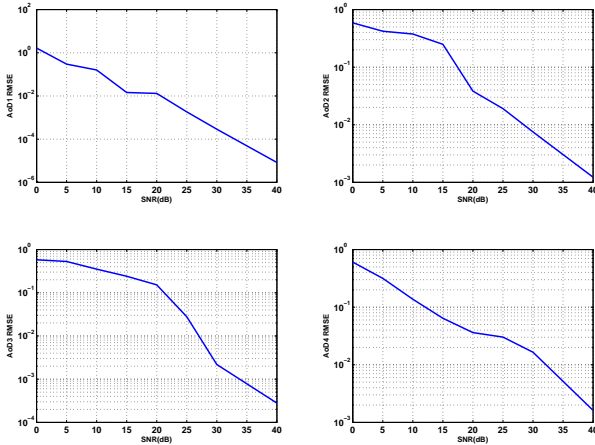


Fig. 3. RMSE of  $\sin(\psi)$

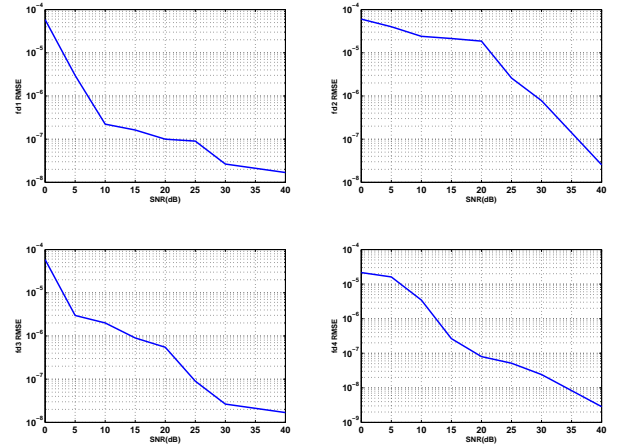


Fig. 5. RMSE of  $\Delta tf_d$

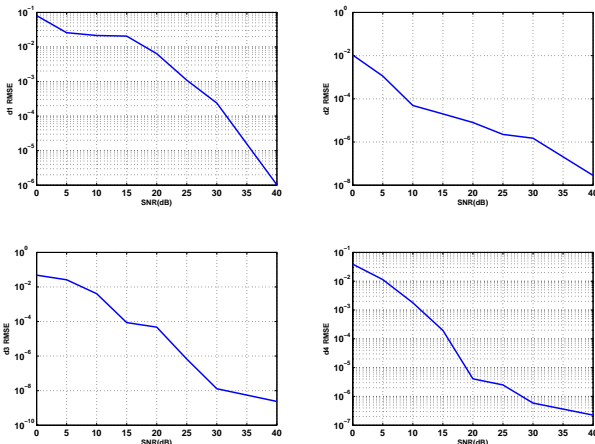


Fig. 4. RMSE of  $\Delta f\tau$

where the terms  $\mu_{ir}$  depend on the LMDP according to

$$\mu_{ir} = \frac{2}{\pi} \arctan(\omega_{ir}), \quad 1 \leq i \leq N_s, \quad 1 \leq r \leq 4. \quad (48)$$

In figures 2-5 we plot the RMSE defined in 47 versus the Signal-to-Noise Ratio (SNR) at the receiver, which is given by

$$SNR = 10 \log_{10} \left( \frac{E\{tr((\bar{\mathbf{H}}\bar{\mathbf{I}})(\bar{\mathbf{H}}\bar{\mathbf{I}})^\dagger)\}}{E\{tr(\bar{\mathbf{N}}\bar{\mathbf{N}}^\dagger)\}} \right) \quad (49)$$

## VI. CONCLUSIONS

In this work we have presented an efficient way to perform the first step of a localization procedure, namely the estimation of the LMDP. We considered a MIMO-OFDM system and we transformed the CIR matrix into a rotation invariant one, by simple concatenation and vectorization operations. The invariance property of the newly formed CIR matrix allowed us to implement a 4-D Unitary ESPRIT algorithm and estimate four different subsets of LMDP simultaneously. The performance

of the algorithm was demonstrated for  $2 \times 4$  system in a NLoS environment with four strong signal components. Results show that the RMSE of the estimates are very small even for small to medium SNR (5 – 10dB). This excellent performance along with its low computational cost make this algorithm an attractive solution to any LMDP estimation problem.

## REFERENCES

- [1] H. Miao, K. Yu, and M. J. Juntti, "Positioning for NLOS Propagation: Algorithm Derivations and Cramer-Rao Bounds," *IEEE Trans. Veh. Technol.*, vol. 56, no. 5, pp. 2568 – 2580, 2007.
- [2] K. Papakonstantinou and D. Slock, "NLOS Mobile Terminal Position and Speed Estimation," in *Proc. 3rd International Symposium on Communications, Control and Signal Processing*, Mar. 2008.
- [3] R. Roy and T. Kailath, "ESPRIT-Estimation of Signal Parameters via Rotational Invariance Techniques," *IEEE Trans. Acoust., Speech, Signal Processing*, vol. 37, no. 7, pp. 984 – 995, 1989.
- [4] A. van der Veen, P. Ober, and E. Deprettere, "Azimuth and Elevaition Computation in High Resolution DOA Estimation," *IEEE Trans. Signal Processing*, vol. 40, no. 7, pp. 1828 – 1832, 1992.
- [5] A. van der Veen, M. Vanderveen, and A. Paulraj, "Joint Angle and Delay Estimation Using Shift-Invariance Techniques," *IEEE Trans. Signal Processing*, vol. 46, no. 2, pp. 405–418, 1998.
- [6] K. T. Wong and M. D. Zoltowski, "Closed-Form Multi-Dimensional Multi-Invariance ESPRIT," Apr. 1997, proc. IEEE International Conference on Acoustics, Speech and Signal Processing 1997.
- [7] M. Haardt and J. Nosske, "Unitary ESPRIT: How to Obtain Increased Accuracy with a Reduced Computational Burden," *IEEE Trans. Signal Processing*, vol. 43, no. 5, pp. 1232 – 1242, 1995.
- [8] —, "Simultaneous Schur Decomposition of Several Nonsymmetric Matrices to Achieve Automatic Pairing in Multidimensional Harmonic Retrieval Problems," *IEEE Trans. Signal Processing*, vol. 46, no. 1, pp. 161–169, 1998.
- [9] H. Miao, K. Yu, and M. J. Juntti, "2-D Unitary ESPRIT Based Joint AOA and AOD Estimation for MIMO System," in *Proc. IEEE 17th International Symposium on Personal, Indoor and Mobile Radio Communications*, Sep. 2006.
- [10] R. R. Muller, "A Random Matrix Model of Communication Via Antenna Arrays," *IEEE Trans. Inform. Theory*, vol. 48, no. 9, pp. 2495 – 2506, 2002.
- [11] K. Papakonstantinou and D. Slock, "Direct Location Estimation using Single-Bounce NLOS Time-Varying Channel Models," in *Proc. IEEE 68th Vehicular Technology Conference*, Sep. 2008.